Environmental Science and Pollution Research (2021) 28:4136–4146
https://doi.org/10.1007/s11356-020-10476-x

RESEARCH ARTICLE

Mitigation of arsenic accumulation in arugula (*Eruca sativa* Mill.) using Fe/Al/Zn impregnated biochar composites

Runze Sun [1] · Jie Wang [2] · Yutao Peng [2] · Hongmei Wang [1] · Qing Chen [2]

Received: 20 May 2020 / Accepted: 10 August 2020 / Published online: 15 September 2020

Abstract

Arsenic (As) contamination of aquatic and soil environments is a global concern, highlighting the importance of As removal via high-efficiency and low-cost removal technologies. In the present study, novel trimetallic biochar was developed through pyrolyzing corn straw impregnated with inexpensive metal Fe/Al/Zn (hydr)oxides. The results of SEM, FTIR, and XRD verified the formation of metal oxyhydroxides on the surface of the modified biochars, and the modification increased the specific surface area (SSA), total pore volume (TPV), and surface charge of the Fe/Al/Zn (hydr)oxides modified biochar (FAZ-CB). Compared with the original biochar, higher sorption rates and capacities was observed for the FAZ-CB. The maximum As (V) adsorption capacities of FAZ-CB reached 82.9 mg g^{-1}. A pot experiment showed that application of FAZ-CB decreased bioavailable As fractions in the red soil significantly reduced the uptake of As by arugula in edible part and root (42.6 and 56.8%, respectively). The present study demonstrated the superiority of FAZ-CB in the As(V) immobilization in red soil, suggesting that it is a promising candidate for practical application for As immobilization. Therefore, FAZ-CB can be used as a promising functionalized biochar to remediate As contaminated red soil.

Keywords Modified biochar · Metal hydroxides · Adsorption · Arsenate · Agricultural wastes · Soil remediation

Introduction

Due to its high toxicity and carcinogenicity, arsenic (As) has been recognized as a group 1 carcinogen by the International Agency on Research Cancer (International Agency for Research on Cancer 2004). Previous studies indicated that chronic exposure to As may affect all of the organs and systems of the human body (Kabir and Chowdhury 2017). As is mainly introduced to the environment via anthropogenic activities, including mining, fossil fuel combustion, and pesticide usage (Gao et al. 2020). In As-affected areas, the high concentrations of As in soil or irrigation water may lead to an elevation in As concentration in cereals, vegetables, or other crop products, potentially causing harmful effects on human health (Guan et al. 2020; Liu et al. 2020a). Therefore, the remediation of the As-polluted waterbody and soil is urgent and has attracted wide interest within environmental research and engineering.

Biochar, a carbonaceous material obtained via conversion of agricultural wastes and by-products, has received increasing attention due to its benefits in agricultural and environmental contexts (Xiang et al. 2019, 2020). A great number of studies have reported that application of biochar in soil can potentially increase soil quality, decrease the bioavailability of organic or inorganic contaminants, and promote plant growth (Gao et al. 2019). In addition, the complex porous structure, high specific surface area, and various functional groups make biochar a widely used material for heavy metal remediation (Yang et al. 2020). However, due to the predominant negative charge on the surface of the biochars, previous studies reported that biochar may have low capability of immobilizing As from soil because the most common species

Responsible Editor: Zhihong Xu

Electronic supplementary material The online version of this article (https://doi.org/10.1007/s11356-020-10476-x) contains supplementary material, which is available to authorized users.

✉ Jie Wang
wangjie321@gmail.com

✉ Qing Chen
qchen@cau.edu.cn

[1] College of Science, China Agricultural University, Beijing 100193, China

[2] College of Resources and Environmental Sciences, China Agricultural University, Beijing 100193, China

of As in porewater existed as anions, i.e., arsenate ($H_2AsO_4^-$, As(V)) and arsenite (H_3AsO_3, As(III)) (Du et al. 2019). Thus, the modification methodologies of conventional biochar for enhancement of As immobilization or removal need further investigation.

To date, diverse techniques and materials have been developed to produce modified biochar with enhanced sorption ability to As (Gao et al. 2020). In particular, modification with metal oxyhydroxides (e.g., iron oxide, manganese oxide, and aluminum oxide) can strongly increase the sorption efficiency of biochar. For example, He et al. (2018) found that the γ-Fe_2O_3-impregnated biochar, fabricated via thermal pyrolysis of corn straw and $FeCl_3$, exhibited excellent As(V) adsorption efficiency of 6.80 mg g^{-1} compared with 0.017 mg g^{-1} for unmodified biochar. Using biochar as soil amendments to decontaminate As bioavailability and the As content in plant tissues has been reported. For instance, applying Fe amendments (such as iron, zero-valent iron, and iron-(hydr)oxide) with biochar can regulate As uptake because a reduction in mobility and bioavailability of As in soil (Lebrun et al. 2019; Qiao et al. 2018). Modification of biochar with a secondary metal has been extensively studied to improve its sorption ability. Wang et al. (2015) found that Fe–Mn bimetal biochar composites showed better As(V) sorption ability (3.44 mg g^{-1}) than single metal-modified biochar, which may be due to the presence of the two metal oxides (MnO and Fe_2O_3) and the bimetal oxides ($MnFe_2O_4$). Similarly, Fe/Mn modified biochar could reduce As mobility in paddy soil and transfer to rice (Lin et al. 2019, 2017). Evidence shows that the enhanced reactivity and sorption ability can be found in the trimetal-based materials (Liu et al. 2019a; Lu et al. 2018; Xu et al. 2019). For example, $Mg_7Zn_1Fe_4$-Asp-LDH showed good adsorption performances for both arsenate and arsenite in aqueous solutions, and the maximum adsorption capacity of As(III) and As(V) reached 94.81 and 57.42 mg g^{-1}, respectively (Lu et al. 2018). In addition, rare earth metal oxides, e.g., lanthanum and cerium, were introduced into the composites to further enhance the As sorption capacity of the bimetal modified biochars because of their superior affinity to As (Liu et al. 2019a; Wang et al. 2016). However, the high cost of rare earth metals precludes their large-scale use as sorbents. Further modification of biochar should consider the metal oxyhydroxides with low cost and excellent As sorption capacity to achieve practical application.

In our previous study, the biochars modified with the Fe/Al (hydr)oxides, which are ubiquitous in aquatic and soil environments, were found to show high capacity for phosphorus adsorption (Peng et al. 2019). Due to the physico-chemical similarity between As and phosphorus, the Fe/Al (hydr)oxide modified biochar may be used as an efficient sorbent for remediating As-polluted soil (Yang et al. 2019). In addition, zinc (hydr)oxides, with advantages of simple production, low cost, and low ecological toxicity, have shown great adsorption capacity for As (Van Vinh et al. 2015). It was reported that the presence of zinc (hydr)oxides in the porous adsorbents, such as LDHs, metal-organic framework, and biochar (Lu et al. 2018; Baghayeri et al. 2020; Zafar et al. 2017), had increased the adsorption capacity for arsenic. Thus, the As adsorptive properties of the modified biochar doped with zinc are worth investigating (Vikrant et al. 2018). In the present study, the primary aim was to fabricate a zinc doped trimetallic biochar by making up the defect of pristine biochar for anion adsorption/immobilization, which can be utilized as a cost-effective and optimal option for As removal in aqueous systems and As-contaminated soil remediation. Various solid-state analysis methods were used to characterize the trimetallic biochar and the sorption performance for As(V) was investigated in aqueous solution. Furthermore, the speciation fractionation and the accumulation in plant tissues were evaluated in parallel in the soil amended with the trimetallic biochar. The hypothesis was that this novel biochar can decrease the available fraction of As in soil and reduce the tissue accumulation.

Materials

Feedstocks and reagents

Corn stalks (Shangzhuang experimental station, Beijing) were selected as feedstock for the biochar preparation. The fresh waste was air-dried before storage, further dried at 105 °C for 24 h, and sieved through a 2-mm mesh before use.

Sodium arsenate dibasic heptahydrate ($Na_2HAsO_4{\cdot}7H_2O$) obtained from Sigma Aldrich (Saint Louis, America) was used to prepare the As(V) stock solution at 200 mg L^{-1} and was diluted with aqueous $NaNO_3$ (0.05 mol L^{-1}) to prepare fresh working solution. Other reagents including iron sulfate ($Fe_2(SO_4)_3$), aluminum sulfate ($Al_2(SO_4)_3$), zinc sulfate heptahydrate ($ZnSO_4{\cdot}7H_2O$), granular sodium hydroxide (NaOH), concentrated hydrochloric acid (HCl), and sodium nitrate ($NaNO_3$) were of analytical grade and purchased from Shanghai Aladdin Industrial Co., Ltd., China.

Preparation of pristine and modified biochars

The pristine corn stalk biochar (CB) was produced via pyrolysis of corn stalk in a muffle furnace. Briefly, metal cans filled with dry feedstock powders were heated in a muffle furnace at 10 °C min^{-1} to 600 °C and held for 2 h. The pyrolysis temperature and time were chosen following previous published studies (Wang et al. 2015; Zhu et al. 2016). The products were sieved through a 0.15-mm mesh and stored in desiccators before use.

The modified biochars, including Fe/Al and Fe/Al/Zn oxyhydroxide impregnated biochars, were synthesized via a co-precipitation method. The aqueous solutions containing

0.8 M Fe^{3+}/0.8 M Al^{3+} and 0.8 M Fe^{3+}/0.8 M Al^{3+}/0.2 M Zn^{2+} were used for preparing Fe/Al corn stalk biochars (FA-CB) and Fe/Al/Zn corn stalk biochars (FAZ-CB), respectively. Briefly, 10 mL of 5 mmol L^{-1} hexadecyl trimethyl ammonium bromide (HTAB) and 50 mL of the metal solution were transferred in a 200-mL beaker. It is noteworthy that the HTAB was used to modify the FA-CB and FAZ-CB to facilitate ion exchange between the FA-CB/FAZ-CB and As(V) (Atia 2008). A 5-g aliquot of pristine biochar was slowly added into the solution and the pH was adjusted to 9–10. The slurry was then thoroughly mixed by sonication for 20 min. The product was centrifuged, washed with deionized (DI) water to remove loosely bound salts until the supernatant was pH-neutral, dried at 80 °C, sieved through a 0.15-mm mesh, and stored in desiccators before use.

Characterization of pristine and modified biochars

The Brunauer–Emmett–Teller (BET) specific surface areas and Barrett–Joyner–Halenda (BJH) pore size distribution were determined through nitrogen adsorption–desorption isotherms at 77 K using an automated gas sorption instrument (ASAP 2460; Micromeritics, Shanghai, China). The electrophoretic mobility of biochars was measured using Zetasizer (Nano ZS90, Malvern, UK) with a fixed scattering angle of 90° and the crystal structure was identified using X-ray diffractometer (XRD) equipped with a CuKα radiation source (X'Pert-Pro MPD; Panalytical B.V., Almelo, Holland). A Fourier-transform infrared spectrometer (FTIR, Tensor 27; Bruker, Karlsruhe, Germany) was used to identify the surface functional groups. Surface morphology and distribution of elemental composition were observed using a scanning electron microscope equipped with energy-dispersive X-ray spectroscopy (SEM-EDS, JSM-7610F; JEOL, Tokyo, Japan). The surface valent states of Fe, Al, Zn, C, and O were analyzed by X-ray photoelectron spectroscopy (XPS, PHI 5100; ULVCA-PHI, Kanagawa, Japan).

As(V) adsorption experiments

Adsorption kinetics of As(V) on biochars were examined by mixing 50 mg of the biochar with 20 mL As(V) solution (20 mg L^{-1}) in 50-mL centrifuge tubes. The tubes were then shaken at 180 rpm on a rotary shaker at 25 °C. At appropriate time intervals (0.2, 0.5, 1, 2, 4, 6, 12, 24, and 48 h), the tubes were withdrawn and the mixtures were immediately filtered through 0.45-μm-pore-size nylon membrane filters. The As(V) concentrations in the lipid phase were determined by using inductively coupled plasma optical emission spectrometry (ICP-OES, ICP-7400; Thermo, USA). The concentration in the solid phase (q_t, mg g^{-1}) was calculated as follows (Du et al. 2020a):

$$q_t = \frac{(C_0 - C_t)V}{m} \quad (1)$$

where C_0 (mg L^{-1}) is the initial As(V) concentration, C_t (mg L^{-1}) is the As(V) concentration measured at time t (min), V (L) is the volume of solution, and m (g) is the mass of biochars.

The adsorption kinetics were fitted using pseudo-first order (Eq. 2) and pseudo-second order (Eq. 3) (Zhang et al. 2020b, c):

$$q_t = q_e\left(1 - e^{-k_1 t}\right) \quad (2)$$

$$\frac{t}{q_t} = \frac{1}{k_2 q_e^2} + \frac{1}{q_e}t \quad (3)$$

where q_e (mg g^{-1}) and q_t (mg g^{-1}) are the amount of As(V) adsorbed onto biochars and modified biochars at equilibrium and at time t (min), respectively, and k_1 (min^{-1}) and k_2 (g mg^{-1} min^{-1}) are the adsorption rate constants of pseudo-first order and pseudo-second order, respectively.

The As(V) adsorption isotherms were determined by mixing 50 mg biochar with 20 mL As(V) solutions of different concentrations (0, 5, 10, 15, 25, 50, and 80 mg L^{-1}) in 50-mL centrifuge tubes. The solution pH was adjusted to 6.5 by adding 1 M HCl or NaOH. The tubes were then shaken on a rotary shaker for 24 h at 25 °C to reach equilibrium. The solution was filtrated through a 0.45-μm-pore-size nylon membrane filter, and the concentrations in the supernatant were then determined. The adsorption was calculated by the same method and further fitted using Langmuir (Eq. 4) and Freundlich (Eq. 5) models (Li et al. 2015; Du et al. 2020b):

$$q_e = \frac{K_L q_m C_e}{1 + K_L C_e} \quad (4)$$

$$q_e = K_F C_e^{1/n} \quad (5)$$

where C_e is the equilibrium concentration of As(V) (mg L^{-1}), q_m is the predicted maximum adsorption capacity of As(V) (mg g^{-1}), K_L (L mg^{-1}) and K_F (L mg^{-1}) are the Langmuir and Freundlich constants, respectively, and n indicates adsorption intensity.

The influence of initial pH on adsorption capacity of pristine and modified biochars was investigated in 20 mg L^{-1} As(V) solutions with different pH values (4–9).

FZA-CB applied in actual As-contaminated soil: pot incubation study

Red soil (pH 5.3) was collected from an agricultural field site in Wuzhou, Guangxi Province, China. This soil is considered contaminated with a total As concentration of 63.3 mg kg^{-1}. The sample was air-dried, sieved through a 2-mm nylon sieve, and mixed homogenously before use. A leafy vegetable, arugula (*Eruca sativa* Mill.) was selected as the test species.

Briefly, arugula seeds were germinated in a 25 °C thermostat incubator (Yiheng MGC-300H, Shanghai). Two days later, six arugula seeds with uniform size were transferred to each pot filled with 1 kg of the treated soil. The 28-day incubation experiment comprising four treatments was designed as follows: (1) control, without biochar; (2) pristine corn stalk biochar (CB); (3) Fe/Al/Zn modified biochar (FAZ-CB). The CB treatment was conducted with application of 0.1 wt.% CB and denoted as CB, whereas the FAZ-CB treatments were conducted with application of 0.1 and 1 wt.% FAZ-CB and denoted as FAZ-CB-0.1 and FAZ-CB-1, respectively. Three replicates were used for each treatment. $(CO(NH_2)_2)$ (0.15 g N kg^{-1} soil), $(NH_4)_2HPO_4$ (0.18 g P kg^{-1} soil) and K_2SO_4 (0.12 mg K kg^{-1} soil) were applied as fertilizer and thoroughly mixed. Plant growth experiments were carried out in an incubator (10 h light, 25 °C, and 65% humidity). The pots were placed randomly and their positions were changed weekly. The plants were routinely irrigated with deionized water to maintain soil water content at 60% of water holding capacity. After a 28-day growing period, arugula was harvested and separated into root and edible parts. The plants were washed, dried at 70 °C for 72 h, and ground for further analysis. The soil sample was air-dried, ground, and passed through a 100-mesh sieve before subsequent analysis.

Speciation fractionation of soil As was performed using the sequential extraction procedures suggested by Wenzel et al. (2001). Briefly, 1 g of dried soil was weighed in 50-mL centrifugation tubes and 20 mL of extractant reagents was added into 50-mL centrifuge tubes sequentially (Table S4). The mixtures were shaken in a rotary shaker at 160 rpm and then the suspensions were centrifuged at 3000 rpm for 15 min. Afterwards, all the supernatants were collected and passed through a 0.22-μm filter and determined for the As concentrations. For the analysis of As concentrations in the edible parts and roots of the plants, approximately 1 g of plant sample was weighed and pre-digested in a mixture of concentrated HNO_3–HCl (1:3, *v*/*v*) at room temperature overnight and then digested in a MAR5 microwave digestion system (CEM Corporation, Matthews, NC, USA). Concentrations of As in the extracted or digested solutions were measured by inductively coupled plasma optical emission spectrometry (ICP-OES, iCAP 7600; Thermo Scientific, USA).

Statistical analysis

All measurements were carried out in triplicates and results were presented as mean ± SD. Data were statistically analyzed using the SPSS 17.0 software package (SPSS, Chicago, IL). Statistical differences between different groups were evaluated by one-way ANOVA followed by the least significant difference. Differences were considered statistically significant at $p < 0.05$.

Results and discussion

Characterization of pristine and modified biochars

The physical properties of the biochars, including specific surface area (SSA), total pore volume (TPV), and total micropore volume (TPV_{micro}), are listed in Table 1. The values of SSA, TPV, and TPV_{micro} in FA-CB and FAZ-CB were significantly higher than those in CB. Specifically, the SSA of FA-CB and FAZ-CB was enlarged by ~ 1.5 times of CB, which was probably because the loaded Fe/Al and Fe/Al/Zn (hydr)oxides on the biochar surface supplied larger TPV and TPV_{micro}. Hence, the impregnation of porous metal oxides on the biochar surface could provide more sorption sites for As removal. Further, the Zeta potential of modified biochars at pH 7.0 increased from − 37.1 to 7.84 mV due to positive surface charge of the Fe/Al/Zn (hydr)oxides, which can eliminate the biochars' inherent alkalinity and enhance their adsorption capacity for As through the increased electrostatic interaction (Gao et al. 2020).

The surface morphology of pristine and modified biochars were studied by SEM (Fig. 1). Due to their inherent nature, the surface of pristine biochars was rough and porous. A flaky irregular polygonal structure with inhomogeneous distributed pores and sharp corners was found in CB, which may be due to the higher contents of lignin and cellulose in plant feedstock. The obtained image of FA-CB and FAZ-CB showed that the sorbent surface consisted of numerous aggregations of small particles, probably representing the presence of metal oxides. The EDS analyses also confirmed that the biochar surface was successfully loaded with Fe, Al, and Zn (Table S1).

The XRD patterns of various biochars (Fig. S4) are similar to the usual XRD pattern of pure silicon oxide (SiO_2). The corresponding diffraction peaks can be indexed by a JCPDS X-ray powder diffraction file No. 99-0088. Further, the strength of SiO_2 in CB was the highest, which was related to the strong absorption capacity of plants to Si, so that the raw material contains a higher silicon element (Paye et al. 2018; Peng et al. 2019). In addition, Fig. S4 indicated that the surface of FAZ-CB was amorphous, which was advantageous as it had good adsorption capacity for hematite and goethite (Antelo et al. 2015).

The modification of surface functional groups on the biochars was evaluated by FTIR analysis (Fig. 2). For the modified biochars, the broad adsorption bands observed at around 3430 cm^{-1} were ascribed to the stretching vibrations of –OH and $–NH_2$, whereas the band at about 1640 cm^{-1} was associated with O–H bending vibration, implying the presence of coordinated water molecules. The band at 1100 cm^{-1} corresponded to the C–C=O stretching vibration modes (Tang et al. 2015). The characteristic peaks of metal–oxygen bonds (M–O and M–O–M, where

Table 1 Surface area, average pore size, pore volume, and Zeta potential of various biochars

Product	[a]S_{BET} ($m^2 g^{-1}$)	Total pore volume ($cm^3 g^{-1}$)	Total micropore volume ($cm^3 g^{-1}$)	[b]Zeta potential (mV)	pH
CB	137	0.080	0.058	− 37.1	10.3
FA-CB	183	0.219	0.072	− 6.09	7.15
FAZ-CB	200	0.247	0.081	7.84	7.34

[a] Surface area was calculated with Brunauer–Emmett–Teller (BET) method

[b] Zeta potential was detected under pH 7

M = Fe, Al, or Zn) in the ranges of 730–476 cm^{-1} suggested the presence of metal oxyhydroxides on the surface of modified biochars (Maji et al. 2018), showing higher intensity in FAZ-CB than CB and FA-CB. These metal–oxygen bonds and oxygen-containing functional groups on biochar surface may play an important role in As removal as the positive adsorption sites. It is noteworthy that the intensity of the peaks (M–O and –OH) in FAZ-CB was higher than that of FA-CB which implied the more abundant functional groups existed in FAZ-CB (Liu et al. 2020b).

The chemical compositions of modified biochars were further studied via XPS spectra (Fig. 3). Fe 2p spectra of modified biochars can be separated into three peaks at 710.49–710.99, 717.23–718.70, and 724.30–724.58 eV, assigning to FeOOH and/or FeO, α-Fe_2O_3, and Fe_3O_4, respectively (Gong et al. 2013; Kang et al. 2017; Tan et al. 1990; Wang et al. 2017). The peak at 73.43–

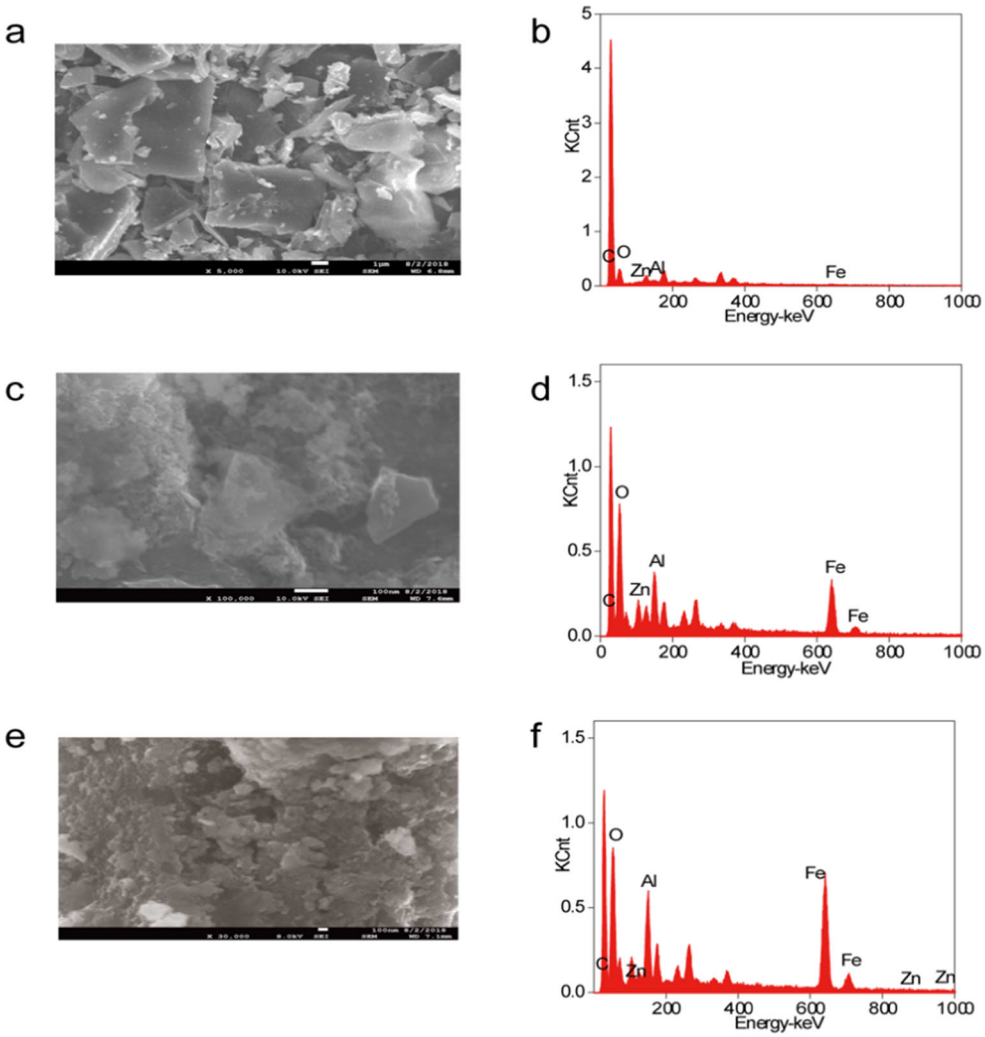

Fig. 1 SEM images of CB (**a**), FA-CB (**c**), and FAZ-CB (**e**); EDS analyses of CB (**b**), FA-CB (**d**), and FAZ-CB (**f**)

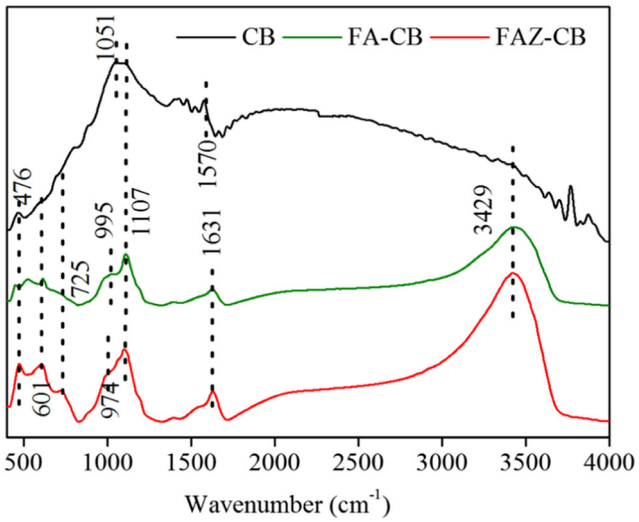

Fig. 2 FTIR spectra of CB, FA-CB, and FAZ-CB

73.97 corresponds to Al element, which may be related to the formation of the more stable alumina (Al_2O_3) fraction (Dieguez-Alonso et al. 2019). The O 1s region (Fig. S5) could be separated into three peaks, suggesting the presence of oxygen-containing functional groups (e.g., O=C and O–C=O), M–O/M–O–H, and M–O–C (where M = Fe, Al, and Zn), respectively (Deng and Ting 2005; Wan et al. 2018), which demonstrated the interaction between metal oxyhydroxide particles and porous carbon.

Effects of pH on As(V) adsorption

To evaluate the effects of pH on As(V) adsorption, the experience of As(V) adsorption by FAZ-CB was investigated with the pH ranging from 3.0 to 9.0 (Fig. S3). The As(V) removal was maintained stable in the acidic and neutral range between pH = 4 and 7, but it was significantly decreased when the initial pH was increased to 8.0 and 9.0, indicating that FAZ-CB was more efficient in the range of the acidic to near-neutral pH for As(V) adsorption.

It was suggested that pH can affect the biochar surface charges by protonation and deprotonation of hydroxyl (–OH) group. Among the four As(V) forms (H_3AsO_4, $H_2AsO_4^-$, $HAsO_4^{2-}$, and AsO_4^{3-}), $H_2AsO_4^-$, and $HAsO_4^{2-}$ were the dominant species at pH 4.0–7.0 and 7.0–9.0, respectively (Wang et al. 2015). When the pH values increased, deprotonation of –OH tended to create a negative charge on biochar surface and repel $H_2AsO_4^-$ and $HAsO_4^{2-}$, thus decreasing As(V) adsorption. In addition, solution pH may change the surface species of mineral elements, and thus impact on the surface changes of the sorbents. For example, the increasing pH may reduce the surface positive charges of FA-CB and FAZ-CB.

Adsorption performance of biochars

Adsorption kinetics were adopted to evaluate biochar's adoption performance and mechanisms for As(V). The adsorption increased with contact time initially and reached apparent equilibrium at 24 h for pristine biochars. In comparison, the time for all modified biochars reaching equilibrium was less than 8 h, indicating that modification by Fe/Al or Fe/Al/Zn can significantly enhance the As(V) adsorption of biochars. As shown in Fig. S1, sharp and rapid initial sorption was obtained, which may be due to the abundance of binding sites and As(V) in the aqueous medium. In this stage, the adsorption of As(V) may be through external surface adsorption or rapid boundary layer diffusion. Subsequently, a much slower phase of the adsorption was observed, which may be ascribed to a peculiar and irretrievable chemisorption or associated to the formation of inner layer complexes (Mohan et al. 2014; Liu et al. 2019b).

The results of fitting relative parameters of pseudo-first-order and pseudo-second-order models are summarized in Table 2. Previous studies indicated that the rate-limiting steps of pseudo-first-order models and pseudo-second-order models were physical adsorption and chemisorption (e.g., electron exchange), respectively. Both models offered well coefficients ($R^2 > 0.983$) which indicated that As(V) was retained with multiple possible mechanisms. Furthermore, the sorption rates for FAZ-CB were 13.4 and 6.09 h^{-1}, respectively, for first-order and second-order models, which were obviously higher than the values of FA-CB (12.0 and 4.54 h^{-1}) and CB (0.189 and 0.113 h^{-1}), which may be attributed to the modification in physicochemical properties.

The fitted parameters of the adsorption-isotherm results are listed in Table 2. The experimental data were fitted well with both Langmuir and Freundlich models ($R^2 > 0.91$). In particular, the fitted results were better for the Langmuir model, with the values of R^2 ranging 0.962–0.976. The good fit of our experimental data by the Langmuir and Freundlich models indicated that the binding of As(V) was closely linked to both monolayer and multilayer adsorption. The highest adsorption capacity was found for FAZ-CB (82.9 mg g^{-1}), which was 4.0 and 8.4 times greater than those of FA-CB and CB, respectively. It should be noted that the As(V) adsorption capacity of FAZ-CB outcompeted most of the adsorbents for As removal reported in previous studies (Table S3). Combined with the aforementioned results of adsorption kinetics, FAZ-CB was found to be the best As(V) adsorption material with highest adsorption rate and greatest adsorption capacity, which may be attributed to the relatively large surface area, high Zeta potential, and great pore volume. In addition, in comparison with other modified biochars in previous studies, the As(V) adsorption capacity of FAZ-CB was also better (Table 2), suggesting that FAZ-CB can be potentially used as the high-performance adsorbent for As(V) adsorption. Compared with the Fe/Al (hydr)oxides, the As(V) adsorption capacity was

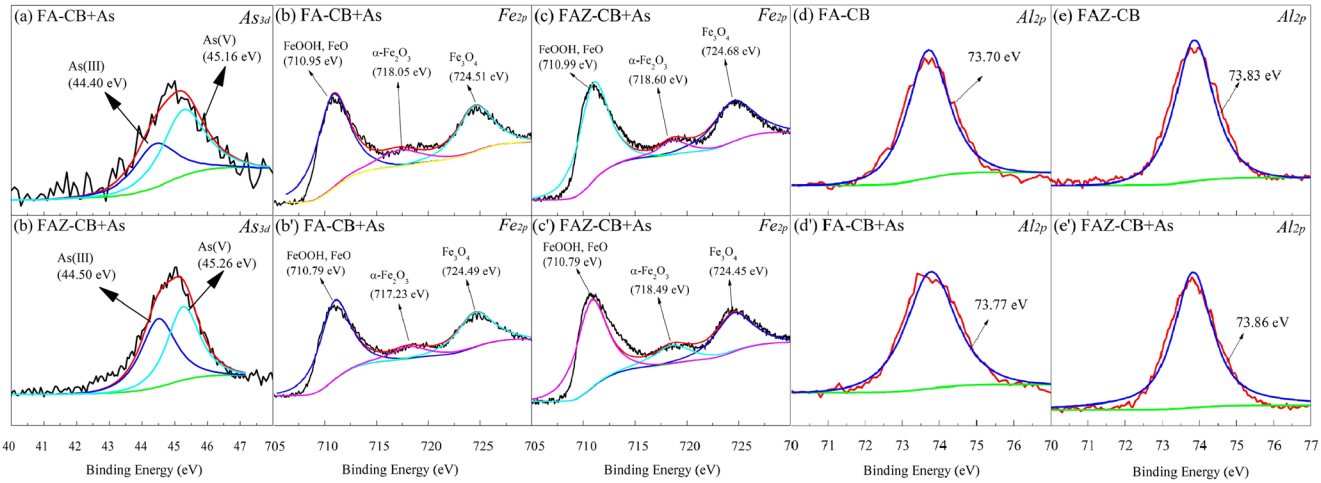

Fig. 3 The XPS spectrum of Fe 2p, Al 2p, and As 3d of modified biochars before and after As(V) adsorption

superior due to the advantages of the Fe–Al–Zn structural interactions in the mixed Fe/Al/Zn hydroxides. The increased adsorption of As(V) on Fe/Al/Zn-binding sites was attributed to the larger SSA with less condensed and less crystalline lattice of the FAZ-CB. The Zeta potential of FAZ-CB (7.84) was higher than that of the Fe/Al (hydr)oxides (− 6.09), indicating that the Zn addition in Fe–Al system favored the increase of the positive charge on the surface of the FA-CB. The greater intensity of hydroxyl groups on the FAZ-CB also contributed to the enhanced coordination with As(V).

To further investigate the mechanism of As(V) adsorption on biochars, the shifts in XPS spectra were examined after sorption experiments. Two separate peaks of post-sorption FA-CB and FAZ-CB biochars were identified in the As3d region, with binding energies of 45.3 and 44.4 eV, respectively. Previous studies have suggested that 3d binding energy was 45.5 eV for As(V) and 44.2 eV for As(III). Therefore, the results of As3d binding energy on the surface of modified biochars may indicate that the As(V) in the initial solution was partly converted into As(III) during the sorption process. Hu et al. (2015) also reported the reduction of As(V) to As(III) on the surface of iron impregnated biochar. The binding energy of 710–711 eV (FeOOH and/or FeO) of 2p indicates that both Fe^{2+} and Fe^{3+} should exist (Li et al. 2011; Zhang et al. 2020a). The binding energy of Fe increased by 0–0.2 eV, suggesting the sorption of As(V) onto FA-CB and FAZ-CB may occur through the combination between the Fe and ligand and the oxidation of Fe^{2+} to Fe^{3+} during the sorption process, which was coupled to the reduction of As(V) to As(III) (Hu et al. 2015). Furthermore, ~ 6.92% increase of Fe^{3+} in the form of Fe_2O_3 (energy position 71.8 eV) was noted on post-adsorption FAZ-CB, which may be also due to the reduction of As(V) during the adsorption (Table S2). A slight positive shift of Al2p spectra was observed after As(V) adsorption, which may be correlated with the interactions between As(V) and Al oxyhydroxides (Lu et al. 2015), including the formation of Al–As and As–O–Al bonds. Given that numerous studies have reported that metal oxyhydroxides and pristine biochars exhibit a certain adsorption capacity, the removal of As(V) in the present study may be mainly through physical adsorption, electrostatic adsorption, and ion exchange (Fig. 4).

The application of FAZ-CB to actual As-contaminated soil

Recently, biochars were applied in soil–water environments for remediation of heavy metal–polluted land (Leksungnoen et al. 2019; O'Connor et al. 2018; Yao et al. 2019; Zama et al. 2018). It is crucial to test functionalized biochar in field environmental conditions, especially in soil environment. Biochar's liming effect can lead to the rise in soil pH, which can greatly reduce the mobility and bioavailability of some cationic heavy metals (*e.g.*, Cd^{2+}, Zn^{2+}, Pb^{2+}), but increase the bioavailability of the anionic metalloids (e.g., arsenate or arsenite) mainly by increasing the net negative charge of variably charged soil constituents (Qiao et al. 2018). As the FAZ-CB shows most superior performance in As(V) adsorption within a wide pH range (4–7), the FAZ-CB was selected for remediation of the As-contaminated soil. In terms of the application dosage, our previous pot experiment result showed that application of 0.1 and 1% biochar is cost-effective and efficient in As-polluted soil remediation (Tang et al. 2020).

Data on As distribution in different parts of arugula (i.e., edible part and root) are shown in Fig. 5. Compared with the CK, in the CB amendment, the As concentration in the edible parts and roots (2.38 and 48.7 mg kg^{-1}, respectively) was significantly increased. The concentration of As was much higher in the roots than that in the edible parts. A higher accumulation of As in the roots was associated with a low translocation toward the upper parts, as observed in previous studies (Beesley et al. 2014; Puckett et al. 2012). Conversely, after the application of the same amount of FAZ-CB (FAZ-CB-0.1), the As concentrations in the

Table 2 Parameters of kinetic models and isotherm models for As(V)

Kinetic models	Adsorbent	Pseudo-first order			Pseudo-second order		
		q_e (g kg^{-1})	k (h^{-1})	R^2	q_e (g kg^{-1})	k (h^{-1})	R^2
	CB	1.36	0.189	0.988	1.68	0.113	0.983
	FA-CB	6.95	12.0	0.998	7.04	4.54	0.999
	FAZ-CB	6.71	13.4	0.997	6.88	6.09	0.998
Isotherm models	Adsorbent	Langmuir			Freundlich		
		q_m (mg g^{-1})	K_L (×10^{-2} L mg^{-1})	R^2	K_F (mg g^{-1}) (L mg^{-1})$^{-1/n}$	n	R^2
	CB	9.92	3.85	0.976	0.97	1.03	0.913
	FA-CB	20.6	2.35	0.974	1.08	0.93	0.956
	FAZ-CB	82.9	0.40	0.962	0.53	1.91	0.968

edible parts and roots decreased significantly. The As concentrations in FAZ-CB-0.1 was 1.42 mg kg^{-1} for edible parts and 25.9 mg kg^{-1}for roots, respectively. The As levels in roots were significantly decreased in FAZ-CB treatments, while the As in the edible parts showed no statistical significance with the control. The aforementioned phenomenon can be ascribed to the widespread plant self-protection (Wang et al. 2019; Liu et al. 2019c). Comparing the treatments provides evidence on efficacy of FAZ-CB for As immobilization and accumulation in plant, which can be contributed to the fact that the addition of FAZ-CB can reduce available As concentrations in red soil. It was reported that $(NH_4)_2SO_4$-As and $NH_4H_2PO_4$-As suggested the bioavailable As in the soil, while Oxalate-As represented the less bioavailable As (Baumann and Fisher 2011). The contents of $(NH_4)_2SO_4$-As and $NH_4H_2PO_4$-As were significantly and positively correlated with As in plants (Qiao et al. 2018). In comparison with the CK, Oxalate-As and Oxalate + ascorbic acid-As for FAZ-CB showed an increasing trend, but there was no significant change for CB (Table 3). Conversely, Oxalate-As showed a significant increasing trend for FAZ-CB-0.1 and FAZ-CB-1 (0.27 and 0.52 mg kg^{-1}, respectively). The finding that the bioavailable As

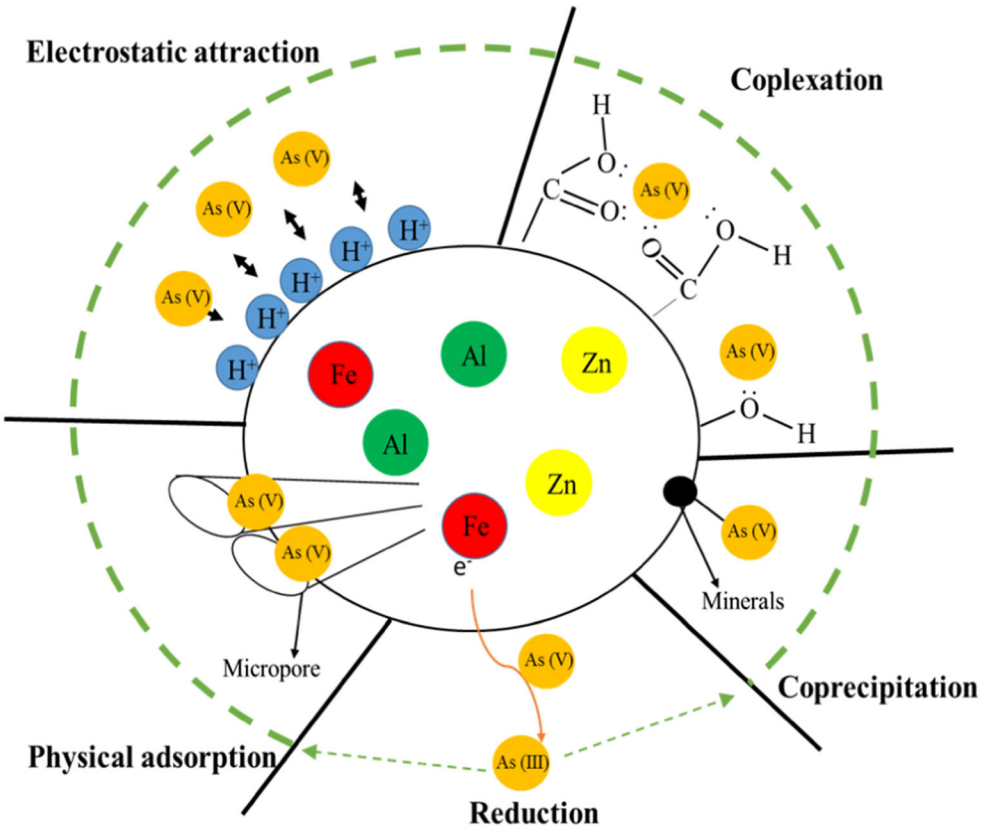

Fig. 4 Conceptual illustration of As(V) sorption processes on FAZ-CB

Table 3 The As fractionation in diverse treatments amended with or without biochar after 28 days' incubation

Treatment	Concentration (mg kg^{-1})				
	$(NH_4)_2SO_4$-As	$NH_4H_2PO_4$-As	Oxalate-As	Oxalate + ascorbic acid-As	HNO_3 +$_2O_2$-As
CK	0.043 ± 0.002a	1.26 ± 0.07a	1.26 ± 0.07c	1.88 ± 0.37b	57.5 ± 3.3a
CB	0.043 ± 0.002a	1.27 ± 0.04a	1.31 ± 0.09c	1.90 ± 0.04b	53.7 ± 5.4a
FAZ-CB-0.1	0.040 ± 0.001a	1.18 ± 0.02b	1.53 ± 0.05b	2.64 ± 0.06a	56.8 ± 2.7a
FAZ-CB-1	0.036 ± 0.002b	1.07 ± 0.03c	1.78 ± 0.11a	2.70 ± 0.11a	61.2 ± 1.8a

Significant differences are indicated by different letters ($P < 0.05$)

was much lower in FAZ-CB-1 than that in CK indicated the FAZ-CB could substantially promote the transformation from bioavailable As into the immobilized fractions (HNO_3 + H_2O_2-As). In the current study, CB was found to have no significant effect on the change of As form in soil. Some researchers (Beesley et al. 2013; Hartley et al. 2009) even observed that the bioavailability of As increased after applying biochar to As-contaminated soil. The reason may be that the effect of biochars for anionic adsorption is closely linked to alkaline pH. Application of biochar was found to increase soil pH, which can greatly enhance the mobility and bioavailability of As by influencing As speciation, dissociation of hydroxyl groups from the surface of the adsorbent, and the dissolution of metal oxides, hydroxides, and carbonates (Houben and Sonnet 2015). Given that As adsorption was mainly influenced by the positive surface charge of the adsorbent (Yang et al. 2010) under strongly acidic conditions, Fe/Al/Zn oxides in FAZ-CB may play a significant role in reducing bioavailable As in soil.

Conclusions

In the present study, tri-metal oxyhydroxide modified biochars were successfully synthesized using low-cost metals and agricultural wastes. The results indicated that Fe/Al/Zn oxyhydroxides significantly increased the specific surface areas, total pore volumes, and Zeta potential values of pristine biochars. The highest maximum adsorption capacity (82.89 mg g^{-1}) was found for Fe/Al/Mn oxyhydroxide modified corn stalk biochar. High pH values in aqueous solution decreased the adsorption of As(V) by Fe/Al/Zn oxyhydroxide modified biochars. In addition, physical adsorption, electrostatic interaction, and inner-sphere complexation may be the main potential mechanisms of As(V) removal. The application of 1% Fe/Al/Zn modified biochars can reduce the As bioavailability in soil and the As uptake by arugula. Long-term effects of the engineered biochars on the soil physical and chemical properties, microecology, and crop yield will be tested to facilitate their future scale-up applications.

Acknowledgment We gratefully acknowledge the financial support of China Agriculture Research System (CARS-23-B16).

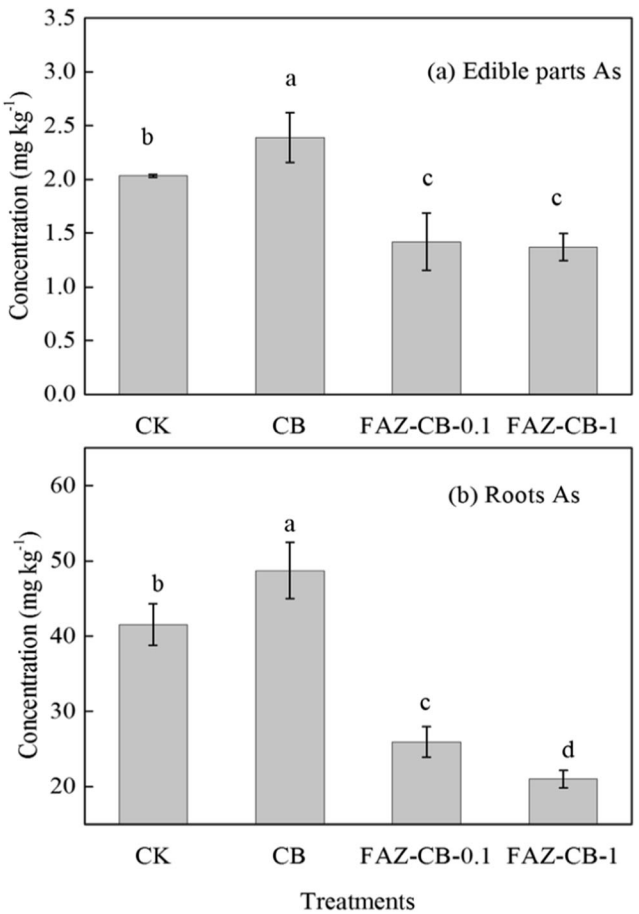

Fig. 5 Effects of CB and FAZ-CB on As concentrations in the plant edible part (**a**) and root (**b**)

References

Antelo J, Arce F, Fiol S (2015) Arsenate and phosphate adsorption on ferrihydrite nanoparticles. Synergetic interaction with calcium ions. Chem Geol 410:53–62

Atia AA (2008) Adsorption of chromate and molybdate by cetylpyridinium bentonite. Appl Clay Sci 41(1-2):73–84

Baghayeri M, Ghanei-Motlagh M, Tayebee R, Fayazi M, Narenji F (2020) Application of graphene/zinc-based metal-organic framework nanocomposite for electrochemical sensing of As (III) in water resources. Anal Chim Acta 1099:60–67

Baumann Z, Fisher NS (2011) Relating the sediment phase speciation of arsenic, cadmium, and chromium with their bioavailability for the deposit-feeding polychaete Nereis succinea. Environ Toxicol Chem 30:747–756

Beesley L, Marmiroli M, Pagano L, Pigoni V, Fellet G, Fresno T, Vamerali T, Bandiera M, Marmiroli N (2013) Biochar addition to an arsenic contaminated soil increases arsenic concentrations in the pore water but reduces uptake to tomato plants (Solanum lycopersicum L.). Sci Total Environ 454–455:598–603

Beesley L, Inneh OS, Norton GJ, Moreno-Jimenez E, Pardo T, Clemente R, Dawson JJC (2014) Assessing the influence of compost and biochar amendments on the mobility and toxicity of metals and arsenic in a naturally contaminated mine soil. Environ Pollut 186: 195–202

Deng S, Ting YP (2005) Polyethylenimine-modified fungal biomass as a high-capacity biosorbent for Cr(VI) anions: sorption capacity and uptake mechanisms. Environ Sci Technol 39:8490–8496

Dieguez-Alonso A, Anca-Couce A, Frišták V, Moreno-Jiménez E, Bacher M, Bucheli TD, Cimò G, Conte P, Hagemann N, Haller AJC (2019) Designing biochar properties through the blending of biomass feedstock with metals: impact on oxyanions adsorption behavior. Chemosphere 214:743–753

Du F, Wang L, Yang ZG, Liu P, Li DL (2019) Ionomic profile and arsenic speciation in Semisulcospira cancellata, a freshwater shellfish from a mine-impacted river in China. Environ Sci Pollut Res 26: 10148–10158

Du Q, Zhang SS, Song JP, Zhao Y, Yang F (2020a) Activation of porous magnetized biochar by artificial humic acid for effective removal of lead ions. J Hazar Mater 389:122115

Du Q, Li GX, Zhang SS, Song JP, Zhao Y, Yang F (2020b) High-dispersion zero-valent iron particles stabilized by artificial humic acid for lead ion removal. J Hazar Mater 383:121170

Gao X, Peng YT, Guo LL, Wang Q, Guan C-Y, Yang F, Chen Q (2020) Arsenic adsorption on layered double hydroxides biochars and their amended red and calcareous soils. J Environ Manag 271:111045

Gao X, Peng YT, Zhou YT, Adeel M, Chen Q (2019) Effects of magnesium ferrite biochar on the cadmium passivation in acidic soil and bioavailability for packoi (Brassica chinensis L.). J Environ Manag 251:109610

Gong J, Yao K, Liu J, Jiang Zw, Chen XC, Wen X, Mijowska E, Tian NN, Tang T (2013) Striking influence of Fe2O3 on the "catalytic carbonization" of chlorinated poly(vinyl chloride) into carbon microspheres with high performance in the photo-degradation of Congo red. J Mater Chem A 1:5247–5255

Guan CY, Chen SS, Lee TH, Yu CP, Tsang DCW (2020) Valorization of biomass from plant microbial fuel cells into levulinic acid by using liquid/solid acids and green solvents. J Clean Prod 260:121097

Hartley W, Dickinson NM, Riby P, Lepp NW (2009) Arsenic mobility in brownfield soils amended with green waste compost or biochar and planted with Miscanthus. Environ Pollut 9

He R, Peng Z, Lyu H, Huang H, Nan Q, Tang J (2018) Synthesis and characterization of an iron-impregnated biochar for aqueous arsenic removal. Sci Total Environ 612:1177–1186

Houben D, Sonnet P (2015) Impact of biochar and root-induced changes on metal dynamics in the rhizosphere of Agrostis capillaris and Lupinus albus. Chemosphere 139:644–651

Hu X, Ding ZH, Zimmerman AR, Wang SS, Gao B (2015) Batch and column sorption of arsenic onto iron-impregnated biochar synthesized through hydrolysis. Water Res 68:206–216

Kabir F, Chowdhury S (2017) Arsenic removal methods for drinking water in the developing countries: technological developments and research needs. Environ Sci Pollut Res 24:24102–24120

Kang BK, Lim BS, Yoon Y, Kwag SH, Park WK, Song YH, Yang WS, Ahn YT, Kang JW, Yoon DH (2017) Efficient removal of arsenic by strategically designed and layer-by-layer assembled PS@ + rGO@GO@Fe3O4 composites. J Environ Manag 201:286–293

Lebrun M, Miard F, Nandillon R, Scippa GS, Bourgerie S, Morabito D (2019) Biochar effect associated with compost and iron to promote Pb and As soil stabilization and Salix viminalis L. growth. Chemosphere 222:810–822

Leksungnoen P, Wisawapipat W, Ketrot D, Aramrak S, Nookabkaew S, Rangkadilok N, Satayavivad J (2019) Biochar and ash derived from silicon-rich rice husk decrease inorganic arsenic species in rice grain. Sci Total Environ 684:360–370

Li P, Jiang EY, Bai HL (2011) Fabrication of ultrathin epitaxial γ-Fe2O3 films by reactive sputtering. J Phys D Appl Phys 44:075003

Li FH, Geng D, Cao Q (2015) Adsorption of As(V) on aluminum-, iron-, and manganese-(oxyhydr)oxides: equilibrium and kinetics. Desalination Water Treat 56:1829–1838

Lin LN, Gao ML, Qiu WW, Wang D, Huang Q, Song ZG (2017) Reduced arsenic accumulation in indica rice (Oryza sativa L.) cultivar with ferromanganese oxide impregnated biochar composites amendments. Environ Pollut 231:479–486

Lin LN, Li ZY, Liu XW, Qiu WW, Song ZG (2019) Effects of Fe–Mn modified biochar composite treatment on the properties of As-polluted paddy soil. Environ Pollut 244:600–607

Liu J, Li N, Zhang WL, Wei XD, Tsang DCW, Sun YB, Luo XW, Bao ZA, Zheng WT, Wang J, Xu GL, Hou LP, Chen YH, Feng YX (2019c) Thallium contamination in farmlands and common vegetables in a pyrite mining city and potential health risks. Environ Pollut 248:906–915

Liu J, Luo XW, Sun YQ, Tsang DCW, Qi JY, Zhang WL, Li N, Yin ML, Wang J, Lippold H, Chen YH, Sheng, GD (2019b) Thallium pollution in China and removal technologies for waters: a review. Environ Intern 126:771–790

Liu J, Ren JM, Zhou YC, Tsang DC.W, Lin JF, Yuan WH, Wang J, Yin ML, Wu Y, Xiao TF, Chen YH (2020a) Effects and mechanisms of mineral amendment on thallium mobility in highly contaminated soils. J Environ Manag 262:110251

Liu J, Ren SX, Cao JL, Tsang DCW, Beiyuan JZ, Peng YT, Fa F, She JY, Yin ML, Shen NP, Wang J (2020b) Highly efficient removal of thallium in wastewater by MnFe2O4-biochar composite. J Hazard Mater 123311

Liu XW, Gao ML, Qiu WW, Khan ZH, Liu NB, Lin L, Song ZG (2019a) Fe–Mn–Ce oxide-modified biochar composites as efficient adsorbents for removing As(III) from water: adsorption performance and mechanisms. Environ Sci Pollut Res 26:17373–17382

Lu HT, Zhu ZL, Zhang H, Zhu JY, Qiu YL (2015) Simultaneous removal of arsenate and antimonate in simulated and practical water samples by adsorption onto Zn/Fe layered double hydroxide. Chem Eng J 276:365–375

Lu HT, Lu TT, Zhang H, Qiu YL, Yin DQ, Zhu ZL (2018) Enhanced adsorption performance of aspartic acid intercalated Mg-Zn-Fe-LDH materials for arsenite. Dalton Trans 47:4994–5004

Maji S, Ghosh A, Gupta K, Ghosh A, Ghorai U, Santra A, Sasikumar P, Ghosh UC (2018) Efficiency evaluation of arsenic(III) adsorption of novel graphene oxide@iron-aluminium oxide composite for the contaminated water purification. Sep Purif Technol 197:388–400

Mohan D, Sarswat A, Ok YS, Pittman CU (2014) Organic and inorganic contaminants removal from water with biochar, a renewable, low cost and sustainable adsorbent—a critical review. Bioresour Technol, Special Issue on Biosorption 160:191–202

O'Connor D, Peng TY, Zhang JL, Tsang DCW, Alessi DS, Shen Z, Bolan NS, Hou DY (2018) Biochar application for the remediation of heavy metal polluted land: a review of in situ field trials. Sci Total Environ 619–620:815–826

Paye W, Tubana B, Harrell D, Babu T, Kanke Y, Datnoff L (2018) Determination of critical soil silicon levels for rice production in Louisiana using different extraction procedures. Commun Soil Sci Plant Anal 49:2091–2102

Peng YT, Sun YQ, Sun RZ, Zhou YT, Tsang DCW, Chen Q (2019) Optimizing the synthesis of Fe/Al (hydr)oxides-biochars to maximize phosphate removal via response surface model. J Clean Prod 237:117770

Puckett EE, Serapiglia MJ, DeLeon AM, Long S, Minocha R, Smart LB (2012) Differential expression of genes encoding phosphate transporters contributes to arsenic tolerance and accumulation in shrub willow (Salix spp.). Environ Exp Bot 75:248–257

Qiao JT, Liu TX, Wang XQ, Li FB, Lv YH, Cui JH, Zeng XD, Yuan YZ, Liu CP (2018) Simultaneous alleviation of cadmium and arsenic accumulation in rice by applying zero-valent iron and biochar to contaminated paddy soils. Chemosphere 195:260–271

Sizmur T, Fresno T, Akgül G, Frost H, Moreno-Jiménez E (2017) Biochar modification to enhance sorption of inorganics from water. Bioresour Technol, Special Issue on Biochar: Production, Characterization and Applications – Beyond Soil Applications 246:34–47

Tan BJ, Klabunde KJ, Sherwood PMA (1990) X-ray photoelectron spectroscopy studies of solvated metal atom dispersed catalysts. Monometallic iron and bimetallic iron–cobalt particles on alumina. Chem Mater 2:186–191

Tang JC, Lv HH, Gong YY, Huang Y (2015) Preparation and characterization of a novel graphene/biochar composite for aqueous phenanthrene and mercury removal. Bioresour Technol 196:355–363

Tang R, Li G, Sun R, Fan B, Chen Q (2020) Effects of applying soil conditioner on soil arsenic uptake by Eruca sativa Mill. var. sativa in acidic soil. CHINA Veg. 48–53.

Van Vinh N, Zafar M, Behera SK, Park H-S (2015) Arsenic(III) removal from aqueous solution by raw and zinc-loaded pine cone biochar: equilibrium, kinetics, and thermodynamics studies. Int J Environ Sci Technol 12:1283–1294

Vikrant K, Kim K-H, Ok YS, Tsang DCW, Tsang YF, Giri BS, Singh RS (2018) Engineered/designer biochar for the removal of phosphate in water and wastewater. Sci Total Environ 616–617:1242–1260

Wan SL, Wu JY, Zhou SS, Wang R, Gao B, He F (2018) Enhanced lead and cadmium removal using biochar-supported hydrated manganese oxide (HMO) nanoparticles: behavior and mechanism. Sci Total Environ 616–617:1298–1306

Wang SS, Gao B, Li YC, Wan YS, Creamer AE (2015) Sorption of arsenate onto magnetic iron–manganese (Fe–Mn) biochar composites. RSC Adv 5:67971–67978

Wang Z, Shen D, Shen F, Li T (2016) Phosphate adsorption on lanthanum loaded biochar. Chemosphere 150:1–7

Wang P, Tang L, Wei X, Zeng GM, Zhou YY, Deng YC, Wang JJ, Xie ZH, Fang W (2017) Synthesis and application of iron and zinc doped biochar for removal of p-nitrophenol in wastewater and assessment of the influence of co-existed Pb(II). Appl Surf Sci 392: 391–401

Wang DD, Xu ZH, Zhang GS, Xia LM, Dong XY, Li Q, Liles MR, Shao JH, Shen QR, Zhang RF (2019) A genomic island in a plant beneficial rhizobacterium encodes novel antimicrobial fatty acids and a self-protection shield to enhance its competition. Environ Microbiol 21:3455–3471

Wenzel WW, Kirchbaumer N, Prohaska T, Stingeder G, Lombi E, Adriano DC (2001) Arsenic fractionation in soils using an improved sequential extraction procedure. Anal Chim Acta 436:309–323

Xiang YJ, Xu ZY, Wei YY, Zhou YY, Yang X, Yang Y, Yang J, Zhang JC, Luo L, Zhou, Z (2019) Carbon-based materials as adsorbent for antibiotics removal: mechanisms and influencing factors. J Environ Manag 237:128–138

Xiang YJ, Yang X, Xu ZY, Hu WY, Zhou YY, Wan ZH, Yan YH, Wei YY, Yang J, Tsang DCW (2020) Fabrication of sustainable manganese ferrite modified biochar from vinasse for enhanced adsorption of fluoroquinolone antibiotics: effects and mechanisms. Sci Total Environ 709:136079

Xu CH, Pan XY, Fang LP, Li J, Li FB (2019) Enhanced reduction of organic pollutants by Fe/Cu@Pd ternary metallic nanoparticles under aerobic conditions: batch and membrane reactor studies. Chem Eng J 360:180–189

Yang WC, Kan AT, Chen W, Tomson MB (2010) pH-dependent effect of zinc on arsenic adsorption to magnetite nanoparticles. Water Res 44:5693–5701

Yang X, Tsibart A, Nam H, Hur J, El-Naggar A, Tack F, Wang CH, Lee YH, Tsang DCW, OK YS (2019) Effect of gasification biochar application on soil quality: trace metal behavior, microbial community, and soil dissolved organic matter. J Hazar Mater 365:684–694

Yang X, Yu IKM, Tsang DCW, Budarin VL, Clark JH, Wu KCW, Yip ACK, Gao B, Lam SS, Ok YS (2020) Ball-milled, solvent-free Sn-functionalisation of wood waste biochar for sugar conversion in food waste valorisation. J Clean Prod 268:122300

Yao AJ, Ju L, Ling XD, Liu C, Wei XG, Qiu H, Tang YT, Morel JL, Qiu RL, Li C, Wang SZ (2019) Simultaneous attenuation of phytoaccumulation of Cd and As in soil treated with inorganic and organic amendments. Environ Pollut 250:464–474

Zafar M, Van Vinh N, Behera S K, Park H S (2017) Ethanol mediated As (III) adsorption onto Zn-loaded pinecone biochar: experimental investigation, modeling, and optimization using hybrid artificial neural network-genetic algorithm approach. J Environ Sci 54:114–125

Zama EF, Reid BJ, Sun GX, Yuan HY, Li XM, Zhu YG (2018) Silicon (Si) biochar for the mitigation of arsenic (As) bioaccumulation in spinach (Spinacia oleracea) and improvement in the plant growth. J Clean Prod 189:386–395

Zhang SS, Du Q, Sun YQ, Song JP, Yang F, Tsang DCW (2020a) Fabrication of L-cysteine stabilized α-FeOOH nanocomposite on porous hydrophilic biochar as an effective adsorbent for Pb2+ removal. Sci Total Environ 720:137415

Zhang SS, Song JP, Du Q, Cheng K, Yang F (2020b) Analog synthesis of artificial humic substances for efficient removal of mercury. Chemosphere 250:126606

Zhang SS, Du Q, Cheng K, Antonietti M, Yang F (2020c) Efficient phosphorus recycling and heavy metal removal from wastewater sludge by a novel hydrothermal humification-technique. Chem Eng J 394:124832

Zhu NY, Yan TM, Qiao J, Cao HH (2016) Adsorption of arsenic, phosphorus and chromium by bismuth impregnated biochar: adsorption mechanism and depleted adsorbent utilization. Chemosphere 164: 32–40